Pharmaceutical Research (2023) 40:937–949
https://doi.org/10.1007/s11095-023-03482-4

ORIGINAL RESEARCH ARTICLE

Simplifying the Extended Clearance Concept Classification System (EC3S) to Guide Clearance Prediction in Drug Discovery

Mitesh Patel[1] · Julia Riede[2] · Dallas Bednarczyk[1] · Birk Poller[2] · Sujal V. Deshmukh[1]

Received: 18 October 2022 / Accepted: 10 February 2023 / Published online: 1 March 2023

Abstract

Purpose The Extended Clearance Concept Classification System was established as a development-stage tool to provide a framework for identifying fundamental mechanism(s) governing drug disposition in humans. In the present study, the applicability of the EC3S in drug discovery has been investigated. In its current format, the EC3S relies on low-throughput hepatocyte uptake data, which are not frequently generated in a discovery setting.

Methods A relationship between hepatocyte uptake clearance and MDCK permeability was first established along with intrinsic clearance from human liver microsomes. The performance of this approach was examined by categorizing 64 drugs into EC3S classes and comparing the predicted major elimination pathway(s) to that observed in humans. As an extension of the work, the ability of the simplified EC3S to predict human systemic clearance based on intrinsic clearance generated using *in-vitro* metabolic systems was evaluated.

Results The assessment enabled the use of MDCK permeability and unscaled unbound intrinsic clearance to generate cut-off criteria to categorize compounds into four EC3S classes: Class 12ab, 2cd, 34ab, and 34cd, with major elimination mechanism(s) assigned to each class. The predictivity analysis suggested that systemic clearance could generally be predicted within threefold for EC3S class 12ab and 34ab compounds. For classes 2cd and 34cd, systemic clearance was poorly predicted using *in-vitro* systems explored in this study.

Conclusion Collectively, our simplified classification approach is expected to facilitate the identification of mechanism(s) involved in drug elimination, faster resolution of *in-vitro* to *in-vivo* disconnects, and better design of mechanistic pharmacokinetic studies in drug discovery.

Keywords discovery · drug classification · intrinsic clearance; *in-vitro* · permeability

Abbreviations

AFE	Average fold error
AAFE	Absolute average fold error
AO	Aldehyde oxidase
BSA	Bovine serum albumin
BCS	Biopharmaceutical classification system
BDDCS	Biopharmaceutics Drug Disposition Classification System
CES	Carboxylesterase
CL	Clearance
CL_{int}	Intrinsic clearance
CL_{hep}	Hepatic clearance
CYP	Cytochrome P450
DMEM	Dulbecco's Modified Eagle Medium
ECCS	Extended Clearance Classification System
EC3S	Extended Clearance Concept Classification System
ECM	Extended Clearance Model
FBS	Fetal bovine serum
FMO	Flavin-containing monooxygenases
fu_{hep}	Fraction unbound in hepatocyte incubation
fu_{inc}	Fraction unbound in incubation
fu_{mic}	Fraction unbound in microsomal incubation
fu_{p}	Fraction unbound in plasma

Mitesh Patel and Julia Riede are the first two authors contributed equally.

✉ Sujal V. Deshmukh
sujal.deshmukh@novartis.com

[1] Pharmacokinetic Sciences, Novartis Institutes for BioMedical Research, Inc., 250 Massachusetts Avenue 2A/242, Cambridge, MA 02139, USA

[2] Pharmacokinetic Sciences, Novartis Institutes for BioMedical Research, Basel, Switzerland

HBSS	Hank's buffered salt solution
HHep	Human hepatocytes
HLM	Human liver microsomes
IVIVE	*In-vitro* to *–in-vivo* extrapolation
MAO	Monoamine oxidase
MDCK	Madin-Darby canine kidney
MDCK-LE	Low efflux MDCK cell line
P_{app}	Apparent passive permeability
$PS_{inf,pass}$	Passive sinusoidal hepatic uptake
Q_H	Hepatic blood flow
R_b	Blood to plasma ratio
RED	Rapid equilibrium dialysis
SULT	Sulfotransferase
UGT	UDP-glucuronosyltransferase
XO	Xanthine oxidase

Introduction

Drug classification systems have evolved to allow prediction of oral drug absorption, disposition and/or the route and mechanism(s) of elimination. An absorption potential concept was first introduced by Dressman *et al*. [1], which was later refined to quantitatively predict the fraction dose absorbed for orally administered drugs [2]. This concept successfully demonstrated the potential impact of various physicochemical properties on the fraction dose absorbed. Subsequently, the biopharmaceutical classification system (BCS) was proposed that enabled the classification of compounds into four classes as a function of their solubility and intestinal permeability rate [3]. Continuing the evolution of classification systems, a quantitative BCS was developed that showed the importance of dose/solubility ratio along with apparent permeability on the extent of drug absorption [4]. Wu and Benet then proposed a derivative of BCS, the Biopharmaceutics Drug Disposition Classification System (BDDCS), that categorized compounds based on their permeability/extent of metabolism and solubility properties [5]. Classification of compounds into the BDDCS enabled an understanding of drug disposition, route(s) of elimination, transporters effects and drug-drug interactions. Subsequently, Varma *et al*. established the Extended Clearance Classification System (ECCS) using properties including passive permeability, molecular weight, and ionization state to predict the predominant clearance mechanism in early drug discovery and development [6]. The Extended Clearance Concept Classification System (EC3S) was also established to provide a framework for identifying the fundamental mechanism(s) governing the overall drug disposition by metabolism and excretion in humans [7–9].

In early drug discovery, considerable resource is invested to predict the human systemic clearance of new molecular entities as clearance is a major determinant of the clinically efficacious dose. Human liver microsomes (HLM) and hepatocytes (HHep) are routinely used to determine the intrinsic metabolic clearance (CL_{int}), which is scaled and applied to the well-stirred model to predict hepatic clearance in humans [10, 11]. The success of *in-vitro* to *in-vivo* extrapolation (IVIVE) approaches is highly reliant on the rate-limiting step in the drug elimination (driving clearance) as well as on the *in-vitro* system used to measure CL_{int} [10–14]. To this end, the Extended Clearance Model (ECM) concept, describing the contribution of various pathways [sinusoidal uptake, sinusoidal efflux, and CL_{int} (metabolic and/or biliary)] to overall hepatic clearance, was established [9]. Applying the ECM concept enabled a better understanding of the rate-limiting step in hepatic clearance thereby remarkably improving IVIVE in humans [9, 12, 15, 16]. Moreover, the ECM, despite focusing on elimination mechanism(s) governing hepatic clearance, provides indirect estimates of the renal clearance, representing an alternative predominant route of drug elimination [14]. The scope of the ECM thus enables an early understanding of the major elimination route as well as mechanism(s) involved in drug clearance. This understanding is crucial in preclinical development to mitigate or manage clearance liabilities within a project.

The EC3S model categorizes compounds by using the *in-vitro* measured passive sinusoidal uptake ($PS_{inf.pas}$) from suspended HHep and scaled metabolic unbound CL_{int} from HLM to derive a two-by-two matrix with four categories and multiple subcategories (Fig. 1A). Fundamentally, the EC3S model clearly demonstrates that the extent of $PS_{inf.pas}$ dictates the likelihood of drugs to be eliminated by hepatic metabolism and/or excretion in the bile or urine as unchanged parent drug by transporter-mediated processes [14]. The EC3S was developed as a predictive tool for identifying the predominant elimination mechanism(s) and better managing potential drug-drug interaction concerns of development candidates. Accordingly, the EC3S relies on resource intensive/low throughput *in-vitro* assay data (e.g. hepatocyte uptake), which are typically derived too late in the drug development process to meaningfully contribute to drug discovery teams attempting to identify the predominant elimination pathway(s) and to guide *in-vitro* assay selection or optimize structural chemistry to address the appropriate clearance issue(s).

To assist compound classification in drug discovery, two considerations could be made, either shifting the developmental assays into early drug discovery or utilizing data from *in-vitro* assays that are already part of the drug discovery workflow. As the first option would require substantial resource commitment, the second consideration leveraging existing assays in the workflow was considered as more favorable. As described above, the EC3S model leverages $PS_{inf,pas}$ derived from a suspended human hepatocyte uptake assay for establishing a permeability cut-off value for high and low permeable compounds. The analogous high-throughput drug discovery permeability measurement is frequently a transcellular permeability assay (e.g., using

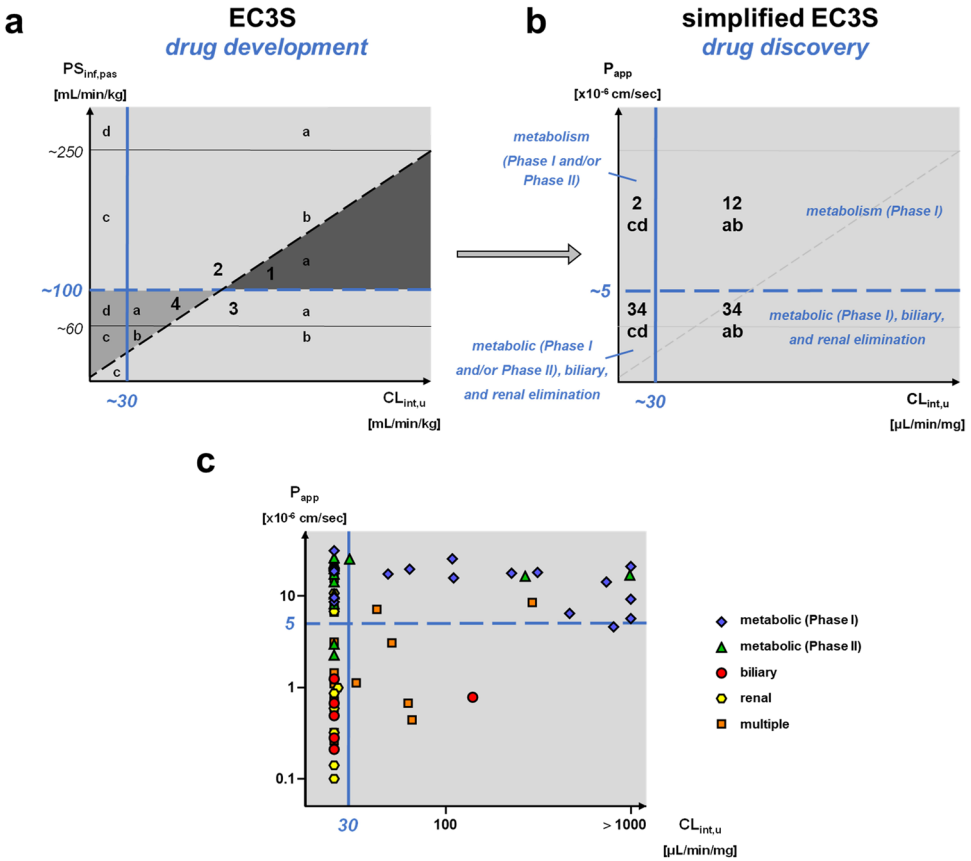

Fig. 1 The Extended Clearance Concept Classification System in drug discovery and development. (**a**) EC3S drug disposition scheme. Dashed blue and black lines indicate the permeability threshold between the EC3S Classes 1/2 and 3/4 ($PS_{inf,pas}=100$ mL/min/kg $\approx 5\times$human Q_H) and the threshold between the EC3S Classes 1/3 and 2/4 ($2\times PS_{inf,pas}=CL_{int,u}$), respectively. Solid lines represent thresholds between the subclasses a, b, c, and d ($PS_{inf,pas} \approx 60$ mL/min/kg, $PS_{inf,pas} \approx 250$ mL/min/kg, and $CL_{int,u} \approx 30$ mL/min/kg). Adapted from Camenisch, 2016 [7]. (**b**) Simplified Extended Clearance Concept Classification System for drug discovery (derived from Fig. 1a). $PS_{inf,pas}$ is replaced by P_{app} [$\times 10^{-6}$ cm/sec] measured in low efflux MDCK cell line (MDCK-LE) and scaled $CL_{int,u}$ (mL/min/kg) was replaced by unscaled $CL_{int,u}$ (µL/min/mg). The dashed horizontal line represents the new threshold of P_{app} (5×10^{-6} cm/sec) between EC3S Classes 1/2 and 3/4 and the solid vertical line represents the threshold of $CL_{int,u}$ (30 µL/min/mg) between EC3S Classes 12ab/34ab and 2cd/34cd, indicating predicted drug disposition and elimination pathways in humans. (**c**) EC3S classes and elimination pathway information of test compounds in the present study (n = 64, Table I). Blue, green, red, yellow, and orange diamonds represent compounds with predominant (≥ 70%) metabolic (Phase I), metabolic (Phase II), biliary, renal, and multiple elimination pathways, respectively. Multiple elimination pathways refer to ≥ two pathways involved, with each contributing to < 70%, to overall drug elimination. $CL_{int,u}$ data > 1000 µL/min/mg were set to $CL_{int,u}=1000$ µL/min/mg, whereas measured $CL_{int,u}$ data are provided in Table I.

Caco-2 or Madin-Darby canine kidney (MDCK) cells). Such monolayer permeability assays are routinely performed in early drug discovery and have previously been used for establishing permeability cut-off values in other classification systems (e.g., ECCS) [6]. In the present study, we have evaluated MDCK permeability, as a surrogate of hepatocyte uptake to categorize compounds into the EC3S classes and determine if the revised classification system appropriately predicts the major elimination mechanism(s). Here, we hypothesized that leveraging such drug discovery data for EC3S class determination would yield predictable route(s) of drug clearance, thereby enabling the identification of the major elimination pathway(s) much earlier in drug discovery. A further objective of the current work was to determine if the simplified EC3S categorization could guide the prediction of *in-vivo* drug clearance.

Materials and Methods

Materials

HLM, liver S9 fractions, and plasma were obtained from Bioreclamation IVT (New York, USA). Human hepatocytes were procured from Celsis (Illinois, USA). Dulbecco's Modified Eagle Medium (DMEM), Leibovitz's L15 medium, fetal bovine serum (FBS) and penicillin/streptomycin were procured from Life Technologies (California, USA). Test

compounds and reagents used in the *in-vitro* assays were purchased from commercial suppliers. All organic solvents and reagents procured from Fisher Scientific (Loughborough, UK and Massachusetts, USA) were of analytical grade and used without any further purification.

Methods

MDCK Permeability

The apparent permeability (P_{app}) of compounds was determined across MDCK-LE (low efflux) cells [17]. Briefly, cells were cultured in DMEM supplemented with FBS (10%), penicillin–streptomycin (100 µg/mL) and Ala-Gln (2 mM). For transport assessments, cells were seeded at a density of approximately 265,000 cells/cm^2 in 96-well Transwell® plates (Corning Life Sciences, Acton, MA) and maintained at 37°C with 5% CO_2 and 95% relative humidity for a period of four days. To initiate transport, media was aspirated, and cells were rinsed thrice with Hank's Balanced Salt Solution (HBSS) supplied with 10 mM HEPES, pH 7.4 (transport buffer). Test compounds (10 µM) in transport buffer containing 0.02% bovine serum albumin (BSA) were added in the apical (donor) chamber whereas the receiver chamber was only filled with transport buffer containing 0.02% BSA. Plates were incubated at 37°C for 120 min without shaking. At the end of the incubation, samples were collected from both donor and receiver chambers and mixed with water:acetonitrile (1:1 v/v) for LC–MS/MS analysis. Bestatin was used as a low permeability marker for monolayer integrity assessments.

Microsomal Metabolic Stability

The metabolic conversion of compounds (1.0 µM) was studied in HLM (0.5 mg/mL) in 100 mM phosphate buffer (pH 7.4) supplemented with 1.0 mM NADPH at 37°C for 30 min. At pre-determined time points (0–30 min), samples were collected and the reaction was terminated with ice-cold acetonitrile. The resulting mixture was centrifuged at 5,000 g for 15 min at 4°C and supernatants were collected for LC–MS/MS analysis. Bosutinib was selected as a positive control to confirm the metabolic activity of the HLM.

Hepatocyte Metabolic Stability

The metabolic stability of compounds (1.0 µM) was determined in suspended HHep (1.0×10^6 viable cells/mL) in Leibovitz's L-15 Medium at 37°C for a period of 80 min. At pre-determined time points, aliquots were collected and the reaction was immediately terminated by addition of ice-cold acetonitrile. Samples were centrifuged at 4,000 g for 10 min at 4°C and the supernatant was analyzed with LC–MS/MS. Verapamil was selected as a positive control to confirm the metabolic activity of HHep.

Hepatocyte Media Loss Assay

For the media loss assay, compounds (0.3 µM) were incubated in suspended HHep (1.0×10^6 cells/mL) in Leibovitz's L-15 Medium at 37°C for 60 min. Samples were withdrawn at pre-determined time points (0–60 min) and centrifuged at 3000 g for 35 s. The supernatant was quenched with an equal volume of ice-cold acetonitrile and samples were analyzed with LC–MS/MS. Verapamil was selected as a positive control to confirm the metabolic activity of HHep.

Liver S9 Metabolic Stability

Test compounds (1.0 µM) were incubated with human liver S9 fractions (2.0 mg/mL) in 100 mM phosphate buffer containing 1.0 mM NADPH, and 2.0 mM $MgCl_2$ at 37°C and 800 rpm for 120 min. At pre-determined time points (0–120 min), samples were taken and immediately quenched with ice-cold methanol and acetonitrile (1:1, v/v). The mixture was centrifuged at 4000 rpm for 30 min at 4°C and the supernatant was analyzed with LC–MS/MS. Midazolam and carbazeran were employed as positive controls to confirm the metabolic activity of liver S9 fractions.

Plasma Protein and Microsomal Binding

The plasma protein binding of compounds was determined in undiluted human plasma using the RED technique. Briefly, following conditioning of the RED Teflon base plate and inserts (Thermo Scientific, Waltham, MA), 300 µL of test compound (5.0 µM) containing fibrin depleted pooled plasma (Bioreclamation, West Sussex, UK) was placed in the plasma chamber while the other chamber was filled with 500 µL of 100 mM phosphate buffer, pH 7.4. Plates were sealed and placed in an incubator maintained at 37°C and 5% CO_2 at 750 rpm for 4 h. At the end of the incubation, matrix was matched for samples withdrawn from both plasma and buffer chambers and immediately quenched with ice-cold acetonitrile. Samples were centrifuged at 2500 g for 15 min and the supernatant was analyzed with LC–MS/MS. An aliquot of plasma spiked with test compounds was collected at time zero to determine % recovery. Bepridil (plasma protein binding $\geq$ 99%) was selected as a positive control.

The microsomal protein binding of test compounds was also measured using RED technique with some modifications. The microsomal protein concentration was 0.5 mg/mL and compounds were tested at 1.0 µM.

Quantitative Analysis

The concentration of compounds in the *in-vitro* samples were quantified using LC–MS/MS technique. The details of the

method employed for sample quantification are described in Supplementary Table I.

Data Analysis

MDCK Permeability

The P_{app} (cm/sec) and %recovery of the compounds was calculated using Eqs. 1 and 2, respectively.

$$P_{app} = (V_R * C_R)/(A * T * D_O) \quad (1)$$

$$\%_{recovery} = 100 * [(C_R + C_D)/D_O] \quad (2)$$

where, V_R is the receiver volume (mL), A is the membrane surface area (0.143 cm^2), D_0 is the concentration of compounds (10.0 µM) at 0 min, C_R and C_D is the compound concentration (µM) in the receiver and donor chamber at 120 min, and T is the time of the study (sec).

In-Vitro CL_{int}

In-vitro CL_{int} in HLM was determined using Eq. 3.

$$CL_{int} = ln2 * \frac{1}{t_{1/2}} * \frac{mL\ incubation}{mg\ microsomal\ protein} \quad (3)$$

where, $t_{1/2}$ is the elimination half-life in min ($t_{1/2}$ = ln2/-slope of the %parent remaining *vs* time plot).

The *in-vitro* CL_{int} (mL/min/mg protein) was scaled using 39.8 microsomal protein per gram liver and 25.7 g liver per kg body weight [18, 19]. The *in-vitro* CL_{int} (mL/min/mg protein) of compounds in liver S9 fractions was also determined using Eq. 3 and further scaled with 121 mg protein per g liver and 25.7 g liver per kg body weight.

The *in-vitro* CL_{int} (mL/min/million cells) of compounds in HHep was calculated using Eq. 4 and scaled with 99 million cells per g liver and 25.7 g liver per kg body weight factors.

$$CL_{int} = ln2 * \frac{1}{t_{1/2}} * \frac{mL\ incubation}{million\ cells} \quad (4)$$

The hepatic CL (CL_{hep}) was predicted using the well-stirred model either uncorrected (Eq. 5) or corrected for plasma protein binding (Eq. 6).

$$CL_{hep} = (Q_H * CL_{int})/(Q_H + CL_{int}) \quad (5)$$

$$CL_{hep} = (Q_H * f_{ub} * CL_{int})/(Q_H + f_{ub} * CL_{int}) \quad (6)$$

where, Q_H is the hepatic blood flow (20.7 mL/min/kg), CL_{int} represents scaled *in-vitro* CL_{int} corrected or uncorrected for incubational binding (fu_{inc}) and fu_b is unbound fraction in the blood. As fu_b values are not routinely measured in early drug discovery, we have assumed $fu_b = fu_p$ ($R_b = 1$) and only fu_p values were used in the well-stirred model to predict the *in-vivo* clearance. As a result, the predicted clearance may not be the true value for compounds whose R_b is considerably > 1 or < 1, respectively. To provide the impact of R_b on clearance predictions, the statistical analysis on the clearance IVIVE with R_b inclusion in the well-stirred model ($fu_b = fu_p/R_b$ in Eq. 6) is provided in the Supplementary Table IV. The R_b values of the 64 test compounds under the present study are provided in the Supplementary Table V.

To correct scaled *in-vitro* CL_{int} from HLM, microsomal binding (fu_{mic}) was used, which was measured for test compounds with logD > 2 or otherwise predicted using the Austin model [20]. Scaled *in-vitro* CL_{int} from HHep and liver S9 fractions was corrected with hepatocyte binding (fu_{hep}), predicted based on the logD/P using the Kilford model [21]. Compounds with CL_{int} < 25 µL/min/mg (lower limit of the HLM incubation) or < 4 µL/min/million cells (lower limit of HHep) indicated negligible to no metabolic turnover and these data were not further corrected with their fu_{inc}.

Plasma Protein and Microsomal Binding

The percent unbound fraction (%fu) was calculated using Eq. 7.

$$\%fu = PAR_B/PAR_M * 100 \quad (7)$$

where, PAR_B and PAR_M represent the peak area ratio (test compound/internal standard) in buffer and the corresponding matrix i.e., plasma (plasma protein binding) or microsomes (microsomal protein binding) after 4 h incubation (equilibrium assumed to be reached), respectively.

Statistical Analysis

The accuracy and precision for IVIVE predictions from different *in-vitro* systems was evaluated using the average fold-error (AFE) and absolute average fold-error (AAFE) as well as using fold-error deviations between the predicted and observed values (% fold error < 3).

$$AFE = 10^{\frac{\sum log\frac{pred}{obs}}{N}} \quad (8)$$

$$AAFE = 10^{\frac{\sum \left|log\frac{pred}{obs}\right|}{N}} \quad (9)$$

Results

Applying MDCK P_{app} in the EC3S for Drug Discovery

To establish a MDCK P_{app} cut-off value that corresponds to the scaled human $PS_{inf,pas}$ value of 100 mL/min/kg, a

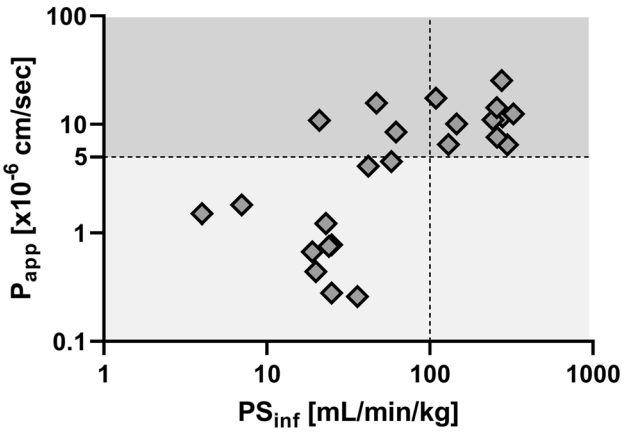

Fig. 2 Categorical alignment between *in-vitro* MDCK-LE P_{app} and sinusoidal hepatocyte $PS_{inf,pas}$ (n = 24 compounds). Permeability data for test compounds are provided in the Supplementary Table II. Dotted lines represent EC3S permeability thresholds of $PS_{inf,pas}$ = 100 mL/min/kg and $P_{app} = 5 \times 10^{-6}$ cm/sec, respectively.

classification alignment between these two parameters was established by measuring the MDCK P_{app} for a series of compounds whose $PS_{inf,pas}$ has previously been generated in suspended human hepatocytes (supplementary Table II, Fig. 2) [16, 22]. A maximized classification alignment (high *vs* low permeability) of 21 out of 24 compounds was achieved for a MDCK P_{app} value of 5×10^{-6} cm/sec as a surrogate for the $PS_{inf,pas}$ cut-off value of 100 mL/min/kg (supplementary Table II). Three compounds (atazanavir, bosentan, and rosiglitazone) were classified as high permeability compounds using MDCK P_{app} value whereas $PS_{inf,pas}$ categorized these compounds as low permeable compounds. The simplified EC3S framework using a MDCK P_{app} cut-off is shown in Fig. 1b.

Implementing MDCK P_{app} and $CL_{int,u}$ into the EC3S for Drug Discovery

To further evaluate the utility of discovery *in-vitro* assays for EC3S compound categorization and elimination pathway prediction, a test set of 64 compounds was selected based on the availability of human clearance data and pathways, with representation across metabolic, renal, biliary, and mixed elimination (Table I). MDCK P_{app} and HLM $CL_{int,u}$ values were determined for these compounds. Based on the values obtained, the compounds were categorized according to the permeability threshold ($P_{app} = 5 \times 10^{-6}$ cm/sec) and measured unbound metabolic clearance ($CL_{int,u}$ = 30 µL/min/mg, which corresponds to a scaled human $CL_{int,u}$ of ~ 30 mL/min/kg after scaling with 39.8 microsomal protein per gram liver and 25.7 g liver per kg body weight). Using these cut-off values, 16 compounds were classified as EC3S Class 12ab, 20 as Class 2cd, 6 as Class 34ab and 22 as 34cd (Fig. 1c and Table I). All compounds that were assigned to the EC3S Class 12ab are eliminated extensively via metabolism mainly by Phase I enzymes in humans. Out of the 20 test compounds assigned to the EC3S Class 2cd, 18 (90%) are eliminated by Phase I and/or II-mediated metabolism in humans. Interestingly, among these 18 test compounds, fleroxacin [23], bisoprolol [24], pitavastatin [25], and moxifloxacin [26] also undergo excretion as unchanged parent (renal and/or bile). Nevertheless, contributory role of Phase I and/or II metabolism in the elimination of these compounds was well predicted with the applied P_{app} and $CL_{int,u}$ thresholds. In line with the EC3S theory, the majority (86%) of the Class 34ab and 34cd compounds undergo substantial renal and biliary excretion or feature mixed elimination pathways (Fig. 1c and Table I).

Clearance Prediction/IVIVE

The CL_{int} of test compounds obtained from incubations with HLM, HHep (stability and media loss assay), and liver S9 fractions (supplementary Table III) was scaled and subjected to the well-stirred model with and without binding corrections to predict the hepatic clearance. Statistical analysis on the clearance predictions from each of these *in-vitro* systems and the correction of binding is summarized in Fig. 3 and Table II. Independent of the EC3S classification and the applied *in-vitro* system, the use of unbound CL_{int} and incorporation of fu_p into the well-stirred liver model yielded the lowest AAFE values and the greatest percent of points within threefold (Fig. 3). Therefore, the subsequent comparative analysis of the clearance predictions from the four *in-vitro* assays (HLM, HHep stability, HHep media loss, or liver S9 fractions) was performed for data utilizing incubational binding and plasma protein binding corrections.

For Class 12ab compounds, under the experimental conditions used to determine CL_{int}, HLM generated the highest fraction of compounds with a measured CL_{int} value above the assay limit (success rate, 100%) as well as reasonable clearance prediction (AAFE < 3.0, with 69% within threefold). For the same set of compounds, the respective AAFE values from HHep and liver S9 fractions were relatively higher (AAFE > 3.0). Moreover, the HHep and liver S9 fractions systems demonstrated a lower success rate than HLM. For EC3S Class 34ab compounds, the clearance was well predicted with either HLM, HHep, or liver S9 fractions (AAFE < 3.0) and clearance predictions were also within threefold error for ≥ 75% of the compounds. Despite a lower number of Class 34ab compounds being tested, HLM was found to have an overall higher success rate (100%) as compared to HHep (67%) and liver S9 fractions (80%).

Class 2cd and 34cd compounds showed very limited metabolic turnover in each of the four *in-vitro* assay setups, as a result, poor IVIVE was observed. The AAFE of

Table I EC3S classification and major elimination pathway information in humans

Compound	P_{app} [10^{-6} cm/sec]	$CL_{int,u}$ [μL/min/mg]	Major elimination pathway	Major mechanism(s)	Ref
EC3S Class 12ab					
Benzydamine	16.5	269	metabolic (Phase I)	FMO, CYP	[46]
Bupivacaine	15.8	111	metabolic (Phase I)	CYP	[47]
Diclofenac	18.1	313	metabolic (Phase I)	CYP	[48]
Imatinib	6.46	468	metabolic (Phase I)	CYP	UW
Luminespib	8.51	294	metabolic (Phase I)	CYP	NP
Lumiracoxib	17.7	227	metabolic (Phase I)	CYP	[49]
Midazolam	21.0	1162	metabolic (Phase I)	CYP	UW
Nicardipine	5.66	10,662	metabolic (Phase I)	CYP	[48]
Nimodipine	9.22	7700	metabolic (Phase I)	CYP	UW
O6-benzylguanine	25.4	30.3	metabolic (Phase I)	AO, XO	[50]
Patupilone	16.9	990	metabolic (Phase I)	CES1	[51]
Propranolol	25.5	108	metabolic (Phase I)	CYP	UW
Quinidine	17.4	49.3	metabolic (Phase I)	CYP	[48]
Nateglinide	7.14	42.3	metabolic (Phase I)	CYP, renal	UW
Venlafaxine	19.7	64.2	metabolic (Phase I)	CYP	UW
Verapamil	14.2	740	metabolic (Phase I)	CYP	UW
EC3S Class 2 cd					
Acetaminophen	8.20	< 25.0	metabolic (Phase II)	UGT, SULT	UW
Antipyrine	19.8	< 25.0	metabolic (Phase I)	CYP	[48]
Betamipron	10.7	< 25.0	renal	renal	[41]
Bisoprolol	22.2	< 25.0	multiple	CYP, renal	UW
Carbazeran	21.9	< 25.0	metabolic (Phase I)	AO, XO	[50]
Citalopram	18.7	< 25.0	metabolic (Phase I)	CYP	UW
Codeine	23.1	< 25.0	metabolic (Phase II)	UGT, CYP	UW
Fleroxacin	6.94	< 25.0	multiple	renal, FMO	[52]
Gatifloxacin	6.78	< 25.0	renal	renal	[39]
Ketoprofen	10.5	< 25.0	metabolic (Phase II)	UGT	[48]
Lorazepam	19.9	< 25.0	metabolic (Phase II)	UGT	UW
Metoprolol	31.3	< 25.0	metabolic (Phase I)	CYP	UW
Moxifloxacin	6.66	< 25.0	multiple	UGT, SULT, bile, renal	[53]
Mycophenolic acid	14.3	< 25.0	metabolic (Phase II)	UGT	UW
Oxazepam	17.4	< 25.0	metabolic (Phase II)	UGT	UW
Pitavastatin	7.60	< 25.0	multiple	UGT, bile	UW
RSV604	8.64	< 25.0	metabolic (Phase I)	CYP	NP
Theophylline	9.60	< 25.0	metabolic (Phase I)	CYP	UW
Vadimezan	15.6	< 25.0	metabolic	CYP, UGT	[54]
Zaleplon	26.1	< 25.0	metabolic (Phase I)	AO, CYP	UW
EC3S Class 34ab					
Aliskiren	0.777	139	biliary	bile	UW
Dacinostat	0.670	62.3	multiple	renal, bile, CYP	NP
Erythromycin	0.437	65.5	multiple	bile, CYP	UW
Etoposide	1.12	32.9	multiple	renal, CYP	[48]
Indinavir	4.59	807	metabolic (Phase I)	CYP	UW
Panobinostat	3.06	51.3	metabolic	CYP, UGT	UW
EC3S Class 34 cd					
Almotriptan	3.12	< 25.0	multiple	CYP, MAO, renal	UW
Cefazolin	0.587	< 25.0	renal	renal	[55]
Cefmetazole	0.317	< 25.0	renal	renal	[56]

Table I (continued)

Compound	P_{app} [10^{-6} cm/sec]	$CL_{int,u}$ [μL/min/mg]	Major elimination pathway	Major mechanism(s)	Ref
Cefodizime	0.992	26.2	renal	renal	[57]
Cefoperazone	0.210	< 25.0	biliary	bile, renal	[58]
Cefpiramide	0.697	< 25.0	multiple	renal, bile	[59]
Ceftizoxime	0.141	< 25.0	renal	renal	[60]
Ciprofloxacin	1.22	< 25.0	renal	renal	[48]
Elinogrel	0.323	< 25.0	multiple	renal, CYP	NP
Famotidine	0.864	< 25.0	renal	renal	[48]
Furosemide	0.754	< 25.0	multiple	renal, UGT	UW
Gavestinel	1.44	< 25.0	metabolic	UGT, CYP	[61]
Napsagatran	0.490	< 25.0	biliary	bile	[62]
Piperacillin	0.0969	< 25.0	renal	renal	[63]
Pravastatin	0.261	< 25.0	multiple	renal, bile	UW
Rosuvastatin	0.279	< 25.0	biliary	bile	UW
Sulfinpyrazone	0.598	< 25.0	multiple	renal, CYP, UGT	[64]
Susalimod	1.24	< 25.0	biliary	bile	[65]
Valsartan	0.674	< 25.0	biliary	bile	UW
Vildagliptin	1.10	< 25.0	multiple	renal, peptidase	[66]
Zidovudine	2.96	< 25.0	metabolic (Phase II)	UGT	[48]
Zoniporide	2.26	< 25.0	metabolic (Phase I)	AO, XO	[67]

$CL_{int,u}$ represents the unscaled intrinsic metabolic clearance from HLM corrected with microsomal binding (fu_{mic}). The fu_{mic} value of above test compounds is provided in the supplementary Table III. Major elimination mechanism refers to the predominant pathway (≥ 70%) likely involved in the elimination of above drugs in humans. Multiple represents ≥ two pathways likely involved, with each contributing < 70% to overall drug elimination. Data on major mechanisms involved in the elimination of above compounds were collected from the University of Washington Drug Interaction Solutions database (UW) or references provided in the table; NP, Data not published (internal data). EC3S, Extended Clearance Concept Classification System; P_{app}, MDCK-LE apparent passive permeability; $CL_{int,u}$, unbound intrinsic clearance; FMO, flavin-containing monooxygenases; CYP, cytochrome P450; AO, aldehyde oxidase; XO, xanthine oxidase; CES, carboxylesterase; UGT, UDP-glucuronosyltransferase; SULT, sulfotransferase; MAO, monoamine oxidase.

hepatic clearance with observed human clearance data was generally poor (AAFE ≥ 3.0) except with liver S9 fractions for Class 2cd compounds (AAFE = 1.84 and 100% compounds within threefold error) and media loss HHep for Class 34cd compounds (AAFE ~ 1.79 and 80% compounds within threefold error). However, only 3 out of 10 (30%) Class 2cd compounds showed measurable CL_{int} in liver S9 fractions, and 4 out of 20 (20%) Class 34cd compounds in the media loss HHep assay. The limited ability to acquire qualified values for Class 2cd and 34cd compounds diminishes the potential utility of these *in-vitro* assay systems to predict the *in-vivo* clearance of these EC3S classes of compounds.

Discussion

Clearance is a major determinant of half-life, oral bioavailability, and dose. Accurate prediction of clearance during the drug discovery and development phases is crucial to guide clinical dose selection and reduce attrition due to poor PK. Since elimination via hepatic metabolism is observed for approximately 70% of marketed drugs [27], *in-vitro* HLM and HHep incubations are frequently used to predict metabolic clearance, guide chemistry on structure-metabolic relationships, and establish IVIVE. In addition to metabolism, hepatic elimination could involve the interplay between sinusoidal uptake, sinusoidal efflux, and biliary secretion. Given the multiplicity of elimination pathways, the ECM concept was introduced to better identify the rate-limiting step and improve hepatic clearance prediction and IVIVE [9, 12, 16]. Subsequently, the EC3S framework was established to better predict the mechanism(s) as well as the contribution of non-hepatic pathway(s) to the overall drug elimination in humans [8, 14].

The structure of the EC3S framework is described in Fig. 1a. As shown, a $PS_{inf.pas}$ cut-off of 100 mL/min/kg (generated using suspended HHep), is used to categorize compounds either into Class 1/2 or 3/4 [7], which would enable the identification of major route(s) of elimination (metabolic and/or secretory). Highly permeable Class 1/2 compounds ($PS_{inf.pas}$ ≥ 100 mL/min/kg) are predominantly

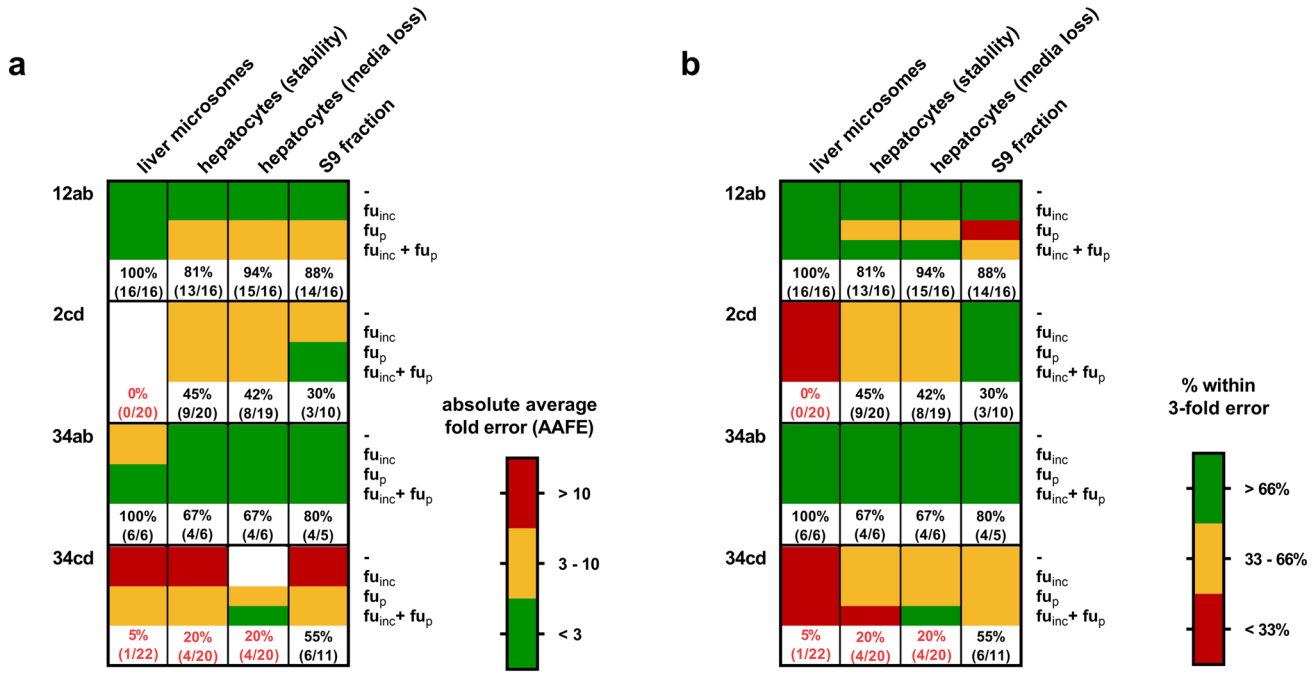

Fig. 3 Accuracy of clearance predictions obtained from different *in-vitro* systems and binding correction methods for each EC3S Class. Colors indicate the absolute average fold error (**a**) and percentage of clearance predictions within a three-fold error (**b**), respectively. Numbers indicate percent of the total number of compounds showing metabolic turnover, above assay limit, in their respective *in-vitro* assays. Numbers are shown in red if turnover for < 30% of compounds was observed. Hepatic clearance was predicted either without consideration of incubational and plasma protein binding (-), under consideration of incubational binding only (fu_{inc}), under consideration of plasma protein binding only (fu_p), or under consideration of both incubational and plasma protein binding ($fu_{inc} + fu_p$).

metabolized in the liver with very limited to no biliary and renal elimination of unchanged drug whereas low permeable Class 3/4 compounds ($PS_{inf.pas} < 100$ mL/min/kg) are found to be substantially cleared as unchanged parent in the bile and urine by transporter-mediated processes. This observation has been previously described in the BDDCS and ECCS, each highlighting the utility of permeability in reflecting the major route of drug elimination in humans [4, 6, 28, 29]. $PS_{inf.pas}$ is not routinely measured in early drug discovery and, as a result, the current EC3S framework offers limited utility for lead optimization. In early drug discovery, permeability of new molecular entities is more frequently evaluated using a high throughput permeability assay e.g. utilizing MDCK or LLC-PK1 cells [30]. Furthermore, MDCK-derived P_{app} data has been shown to reasonably correlate with $PS_{inf,pas}$ measured using suspended HHeps [31], which further supports the use of P_{app} as a surrogate for $PS_{inf,pas}$ in the EC3S framework. The MDCK P_{app} was generated for a set of 24 compounds whose $PS_{inf,pas}$ values were previously generated using suspended HHep [14, 22]. A classification alignment between these two parameters was established using a MDCK P_{app} cut-off of 5×10^{-6} cm/sec, as previously applied in the ECCS by Varma *et al.* [6]. Using a P_{app} cut-off of 5×10^{-6} cm/sec, the majority of compounds were found to be correctly assigned in to the EC3S classes 1/2 or 3/4 (Supplementary Table II). However, atazanavir, bosentan, and rosiglitazone were classified as Class 1/2 instead of Class 3/4 compounds. Previous reports from the literature have shown that these three compounds are moderate to high permeable compounds [31–33], which is in line with the P_{app}-based assignment into Class 1/2 compounds as well as their elimination via metabolism in humans [34–38]. Taken together, these findings clearly demonstrate MDCK P_{app} as a surrogate for $PS_{inf,pas}$ to differentiate new molecular entities into the EC3S classes.

In addition to assessing permeability, high throughput stability assays with HLM are routinely employed to determine metabolic CL_{int} of new molecule entities. Since HLM CL_{int} is readily available in a discovery setting, the utility of this parameter along with MDCK P_{app} to enable compound assignment into the EC3S was further explored. Furthermore, to better incorporate EC3S framework in drug discovery and eliminate the need of species-specific scaling factors, unscaled $CL_{int,u}$ (as opposed to scaled $CL_{int,u}$ (mL/min/kg)) with a cut-off value of 30 µL/min/mg was employed (Fig. 1a, b). As shown in Fig. 1b, using the MDCK P_{app} (5×10^{-6} cm/sec) and HLM $CL_{int,u}$ (30 µL/min/mg) thresholds, compounds could be assigned into the EC3S classes as highly permeable and extensively metabolized mainly by Phase I enzymes (Class 12ab), highly permeable and metabolized by

Table II Statistical analysis on the human clearance predictions using *in-vitro* CL_{int} from HLM, HHep and liver S9 fractions

Method	n	success rate	AFE	AAFE	within threefold
EC3S Class 12ab					
Microsomes	16	100%	0.77	2.49	69%
Hepatocytes (stability)	16	81%	0.46	3.28	69%
Hepatocytes (media loss)	16	94%	0.59	3.04	67%
Liver S9 fractions	16	88%	0.33	3.36	50%
EC3S Class 2 cd					
Microsomes	20	0%	NA	NA	NA
Hepatocytes (stability)	20	45%	0.43	4.16	56%
Hepatocytes (media loss)	19	42%	0.43	4.03	44%
Liver S9 fractions	10	30%	0.89	1.84	100%
EC3S Class 34ab					
Microsomes	6	100%	1.49	1.99	83%
Hepatocytes (stability)	6	67%	0.57	1.75	75%
Hepatocytes (media loss)	6	67%	1.07	1.29	100%
Liver S9 fractions	5	80%	0.71	2.02	100%
EC3S Class 34 cd					
Microsomes	22	5%	3.76	3.76	0%
Hepatocytes (stability)	20	20%	0.58	3.36	25%
Hepatocytes (media loss)	20	20%	0.63	1.79	80%
Liver S9 fractions	11	55%	0.75	4.61	33%

Statistical parameters on the hepatic clearance prediction were determined using the well-stirred liver model corrected for both fu_p and fu_{inc}. "n" represents number of compounds incubated in HLM, HHep, and liver S9 fractions for each EC3S Class, respectively. Success rate represents % of compounds that showed CL_{int} value above the assay limit in the HLM, HHep, and liver S9 fractions and whose predicted human clearance data was used in the statistical analysis for IVIVE. NA represents not applicable for statistical analysis. AFE, average fold-error; AAFE, absolute average fold-error.

Phase I and/or II enzymes (Class 2cd), poorly permeable and eliminated by Phase I enzymes, renal and/or biliary excretion (Class 34ab), and poorly permeable and eliminated by Phase I/II enzymes, renal and/or biliary excretion (Class 34cd). To evaluate the potential of this classification approach, MDCK P_{app} and $CL_{int,u}$ values were determined for a set of 64 test compounds, whose major elimination pathway(s) are known in humans, and assigned to the EC3S classes (Fig. 1c and Table I). Amongst these 64 test compounds, 16 were classified as EC3S Class 12ab (25%), 20 as Class 2cd (~31%), 6 as Class 34ab (~9%), and 22 as Class 34cd (~34%) compounds. While all 16 EC3S Class 12ab compounds were correctly predicted to be predominately eliminated via Phase I metabolism in humans (Table I), 2 out of the 18 EC3S Class 2cd compounds (betamipron and gatifloxacin) are found to be misclassified as these compounds are mainly eliminated as unchanged parent in the urine, via both glomerular filtration and active tubular secretion [39–41], which is uncommon for compounds with moderate to high passive permeability. The number of compounds categorized into the EC3S Class 34ab from the current set was limited (n = 6), with many compounds displaying multiple elimination pathways (Table I). It is noteworthy to mention that indinavir, which is mainly eliminated via Phase I-mediated hepatic metabolism (CYPs) in humans, was assigned to EC3S Class 3/4 as the MDCK P_{app} (4.6×10^{-6} cm/sec) was below the threshold of 5×10^{-6} cm/sec. A recent study reported MDCK P_{app} of 5.4×10^{-6} cm/sec for indinavir using similar assay conditions [42], which would classify this compound into the EC3S Class 12ab that are predominantly eliminated by Phase I enzymes. This finding suggests that for compounds, where the measured assay value approximates the EC3S cut-off criteria, it could be challenging to accurately classify them due to assay variability. Nonetheless, based on our classification model (Fig. 1b), Phase I enzymes are proposed to be involved in the elimination of EC3S Class 34ab compounds, consistent to that observed with indinavir. Lastly, poorly permeable, and low metabolic turnover EC3S Class 34cd compounds were anticipated to undergo substantial urinary and/or biliary excretion, with or without hepatic metabolism, as observed for majority of compounds (19 out of 22) assigned to this EC3S class. Taken together, these observations clearly demonstrate that the modified EC3S classification approach, which uses MDCK P_{app} (5×10^{-6} cm/sec) and HLM $CL_{int,u}$ (30 µL/min/mg) thresholds for compound assignment, could enable an early prediction and understanding of the major elimination pathway(s) for new molecular entities in drug discovery. Moreover, this classification approach has potential to allow prediction of key metabolic pathways such as oxidative and/or conjugative (Phase I for EC3S subclasses a and b *vs* Phase I and II for subclasses c and d) to overall drug elimination in humans.

In addition to employing HLM $CL_{int,u}$ for the EC3S compound assignments, we also investigated clearance IVIVE using this system, in comparison to HHep and liver S9 fractions for the individual EC3S classes. For comparative analysis, HHep was selected as alternative system as it is widely used in a high throughput format to study metabolic stability of compounds in a discovery setting. Moreover, HHep and liver S9 fractions also contain non-CYP enzymes (UGTs, AO, reductases) unlike HLM, whose incubations are often conducted in the presence of NADPH as the only co-factor (no UDPGA) making it more suitable for screening compounds that primarily undergo CYP-mediated metabolism. As such, compounds undergoing metabolism by non-CYP mechanisms and/or being actively transported by sinusoidal transporters (e.g., by OATPs) could display higher CL_{int} in HHep and liver S9 fractions relative to HLM [43]. Amongst these *in-vitro* systems and the assay conditions describe herein, the percentage of EC3S Class 12ab compounds (n = 16) that showed turnover in

HLM was generally higher relative to HHep and liver S9 fractions. Furthermore, IVIVE for EC3S Class 12ab compounds was better with HLM relative to HHep and liver S9 fractions (Table II). Likewise, the metabolic turnover of the total number of EC3S Class 34ab compounds was higher in HLM relative to HHep (stability and media loss assay) and liver S9 fractions. The *in-vivo* clearance of EC3S Class 34ab compounds was well predicted (AAFE < 3 and ≥ 75% compounds within threefold error of the observed clearance) using all three *in-vitro* systems. However, our analysis on the clearance IVIVE for EC3S Class 34ab is limited to a total of six compounds. Taken together, it appears that HLM provides reasonable IVIVE of clearance for EC3S Class 12ab and 34ab compounds (Fig. 3). By contrast, the turnover of EC3S Class 2cd and 34cd compounds in HLM was negligible. Although, a limited number of EC3S Class 2cd and 34cd compounds were metabolically turned over in HHep (≤45%) and liver S9 fractions (≤55%), their IVIVE of human clearance was generally very poor. It is noteworthy to mention that the current IVIVE analysis focuses on the correlation of predicted hepatic clearance (from HLM, HHep or liver S9 fractions) to the total systemic clearance in humans. EC3S Class 34cd compounds are anticipated to undergo substantial renal and/or biliary excretion, which could explain poor IVIVE for this set of compounds. It is noteworthy to mention that the IVIVE approach used in the present study has some limitations. For IVIVE analysis, the well-stirred model has been selected to predict the *in-vivo* hepatic clearance though its limitations compared to other complicated models (parallel tube, dispersion, zonal liver, etc.) have been well described by Pang *et al.* [44]. Moreover, the *in-vitro* CL_{int} obtained from incubations, also defined as an arterial intrinsic clearance by Benet and Sodhi [45], is used to predict the human hepatic clearance, but compared to the observed systemic (or whole-body arterial) drug clearance for IVIVE rather than to the liver organ clearance. Additionally, R_b has been assumed to be unity in the well-stirred model as this parameter is not routinely measured in early drug discovery.

Conclusion

In summary, the present study demonstrates the utility of high throughput MDCK-LE P_{app} (5×10^{-6} cm/sec) and HLM $CL_{int,u}$ data (30 µL/min/mg) to enable EC3S compound classification for drug discovery. Compound assignment into the EC3S classes could provide an early understanding/prediction of the major route of elimination to drug discovery teams. HLM is a robust *in-vitro* system to predict hepatic clearance of compounds in EC3S Class 12ab and 34ab, whereas its utility is very limited for Class 2cd and 34cd compounds. To our surprise, HHep or liver S9 fraction underperformed for Class 2cd compounds, where Phase I and or II enzymes are predominantly involved in drug elimination. This suggests the need for further optimization of assay conditions or alternative *in-vitro* models such as long-term cell culture, extrahepatic systems, or recombinant enzymes for low turnover compounds. Finally, for EC3S Class 34cd compounds, IVIVE based on metabolic *in-vitro* systems is likely to be poor due to substantial contribution of excretory pathways (e.g., renal/biliary clearance). In such cases, the involvement of uptake and efflux transporters (liver and kidney) could be explored. The current framework faces some limitations compared to the use of HHep-derived $PS_{inf.pas}$ for compound categorization. $PS_{inf.pas}$ allows quantitative predictions of hepatic *vs* extrahepatic clearance [9], which is challenging with our proposed approach. Lastly, the present approach applies MDCK-LE P_{app} (5×10^{-6} cm/sec) and $CL_{int,u}$ (30 µL/min/mg) to predict major route(s) of drug elimination and clearance IVIVE for humans. For preclinical species, a re-assessment of these classification cut-offs will be necessary.

Supplementary Information The online version contains supplementary material available at https://doi.org/10.1007/s11095-023-03482-4.

Acknowledgements The authors would like to thank Drs. Gian Camenisch and Bernard Faller for their constructive critique of various aspects of this article. We would also like to thank Gaelle Chenal, PhongHung Nguyen, Gaurab KC, Markus Trunzer, and Linda Xiao for their contribution in *in-vitro* assays. Authors would also like to acknowledge Dr. Rowan Stringer for his help in the data compilation.

Author Contributions Participated in research design: Patel, Riede, Poller.

Conducted experiments: Patel, Riede.

Performed data analysis: Riede, Patel, Deshmukh.

Wrote or contributed to the writing of the manuscript: Patel, Riede, Bednarczyk, Deshmukh.

Data Availability The datasets generated during and/or analyzed during the current study are available from the corresponding author on reasonable request.

Declarations

Conflict of Interest The authors declare no conflicts of interest for this work beyond employment noted in the affiliations.

References

1. Dressman JB, Amidon GL, Fleisher D. Absorption potential: estimating the fraction absorbed for orally administered compounds. J Pharm Sci. 1985;74(5):588–9.
2. Macheras PE, Symillides MY. Toward a quantitative approach for the prediction of the fraction of dose absorbed using the absorption potential concept. Biopharm Drug Dispos. 1989;10(1):43–53.
3. Amidon GL, Lennernas H, Shah VP, Crison JR. A theoretical basis for a biopharmaceutic drug classification: the correlation of in vitro drug product dissolution and in vivo bioavailability. Pharm Res. 1995;12(3):413–20.

4. Wu CY, Benet LZ. Predicting drug disposition via application of BCS: transport/absorption/ elimination interplay and development of a biopharmaceutics drug disposition classification system. Pharm Res. 2005;22(1):11–23.
5. Rinaki E, Valsami G, Macheras P. Quantitative biopharmaceutics classification system: the central role of dose/solubility ratio. Pharm Res. 2003;20(12):1917–25.
6. Varma MV, Steyn SJ, Allerton C, El-Kattan AF. Predicting clearance mechanism in drug discovery: extended clearance classification system (ECCS). Pharm Res. 2015;32(12):3785–802.
7. Camenisch GP. Drug disposition classification systems in discovery and development: a comparative review of the BDDCS. ECCS and ECCCS Concepts Pharm Res. 2016;33(11):2583–93.
8. Kunze A, Poller B, Huwyler J, Camenisch G. Application of the extended clearance concept classification system (ECCCS) to predict the victim drug-drug interaction potential of statins. Drug Metab Pers Ther. 2015;30(3):175–88.
9. Riede J, Kunze A, Huwyler J, Poller B, Umehara K. The extended clearance model and its use for the interpretation of hepatobiliary elimination data. ADMET. 2015;3(1):1–14.
10. Obach RS. The prediction of human clearance from hepatic microsomal metabolism data. Curr Opin Drug Discov Devel. 2001;4(1):36–44.
11. Pang KS, Rowland M. Hepatic clearance of drugs. I. Theoretical considerations of a "well-stirred" model and a "parallel tube" model. Influence of hepatic blood flow, plasma and blood cell binding, and the hepatocellular enzymatic activity on hepatic drug clearance. J Pharmacokinet Biopharm. 1977;5(6):625–653.
12. Camenisch G, Umehara K. Predicting human hepatic clearance from in vitro drug metabolism and transport data: a scientific and pharmaceutical perspective for assessing drug-drug interactions. Biopharm Drug Dispos. 2012;33(4):179–94.
13. Chao P, Uss AS, Cheng KC. Use of intrinsic clearance for prediction of human hepatic clearance. Expert Opin Drug Metab Toxicol. 2010;6(2):189–98.
14. Riede J, Poller B, Umehara K, Huwyler J, Camenisch G. New IVIVE method for the prediction of total human clearance and relative elimination pathway contributions from in vitro hepatocyte and microsome data. Eur J Pharm Sci. 2016;86:96–102.
15. Shitara Y, Sato H, Sugiyama Y. Evaluation of drug-drug interaction in the hepatobiliary and renal transport of drugs. Annu Rev Pharmacol Toxicol. 2005;45:689–723.
16. Umehara K, Camenisch G. Novel in vitro-in vivo extrapolation (IVIVE) method to predict hepatic organ clearance in rat. Pharm Res. 2012;29(2):603–17.
17. Dickson CJ, Hornak V, Bednarczyk D, Duca JS. Using membrane partitioning simulations to predict permeability of forty-nine drug-like molecules. J Chem Inf Model. 2019;59(1):236–44.
18. Zhang H, Gao N, Tian X, Liu T, Fang Y, Zhou J, Wen Q, Xu B, Qi B, Gao J, Li H, Jia L, Qiao Q. Content and activity of human liver microsomal protein and prediction of individual hepatic clearance in vivo. Scientific Reports. 2015;5(1).
19. Davies B, Morris T. Physiological parameters in laboratory animals and humans. Pharm Res. 1993;10(7):1093–5.
20. Austin RP, Barton P, Cockroft SL, Wenlock MC, Riley RJ. The influence of nonspecific microsomal binding on apparent intrinsic clearance, and its prediction from physicochemical properties. Drug Metab Dispos. 2002;30(12):1497–503.
21. Kilford PJ, Gertz M, Houston JB, Galetin A. Hepatocellular binding of drugs: correction for unbound fraction in hepatocyte incubations using microsomal binding or drug lipophilicity data. Drug Metab Dispos. 2008;36(7):1194–7.
22. Riede J, Poller B, Huwyler J, Camenisch G. Assessing the risk of drug-induced cholestasis using unbound intrahepatic concentrations. Drug Metab Dispos. 2017;45(5):523–31.
23. Hayton WL, Vlahov V, Bacracheva N, Viachki I, Portmann R, Muirhead G, Stoeckel K, Weidekamm E. Pharmacokinetics and biliary concentrations of fleroxacin in cholecystectomized patients. Antimicrob Agents Chemother. 1990;34(12):2375–80.
24. ZEBETA® Drug label. 2007.
25. Saito Y. Pitavastatin: an overview. Atheroscler Suppl. 2011;12(3):271–6.
26. AVELOX® Drug label. 2016.
27. Wienkers LC, Heath TG. Predicting in vivo drug interactions from in vitro drug discovery data. Nat Rev Drug Discov. 2005;4(10):825–33.
28. Benet LZ. Predicting drug disposition via application of a Biopharmaceutics Drug Disposition Classification System. Basic Clin Pharmacol Toxicol. 2010;106(3):162–7.
29. Benet LZ. The role of BCS (biopharmaceutics classification system) and BDDCS (biopharmaceutics drug disposition classification system) in drug development. J Pharm Sci. 2013;102(1):34–42.
30. Balimane PV, Chong S. Cell culture-based models for intestinal permeability: a critique. Drug Discov Today. 2005;10(5):335–43.
31. Li R, Bi YA, Lai Y, Sugano K, Steyn SJ, Trapa PE, Di L. Permeability comparison between hepatocyte and low efflux MDCKII cell monolayer. AAPS J. 2014;16(4):802–9.
32. Varma MV, Gardner I, Steyn SJ, Nkansah P, Rotter CJ, Whitney-Pickett C, Zhang H, Di L, Cram M, Fenner KS, El-Kattan AF. pH-Dependent solubility and permeability criteria for provisional biopharmaceutics classification (BCS and BDDCS) in early drug discovery. Mol Pharm. 2012;9(5):1199–212.
33. Kis O, Zastre JA, Hoque MT, Walmsley SL, Bendayan R. Role of drug efflux and uptake transporters in atazanavir intestinal permeability and drug-drug interactions. Pharm Res. 2013;30(4):1050–64.
34. TRACLEER® Drug label. 2017.
35. AVANDIA® Drug label. 2008.
36. REYATAZ® Drug label. 2011.
37. Weber C, Gasser R, Hopfgartner G. Absorption, excretion, and metabolism of the endothelin receptor antagonist bosentan in healthy male subjects. Drug Metab Dispos. 1999;27(7):810–5.
38. Cox PJ, Ryan DA, Hollis FJ, Harris AM, Miller AK, Vousden M, Cowley H. Absorption, disposition, and metabolism of rosiglitazone, a potent thiazolidinedione insulin sensitizer, in humans. Drug Metab Dispos. 2000;28(7):772–80.
39. Nakashima M, Uematsu T, Kosuge K, Kusajima H, Ooie T, Masuda Y, Ishida R, Uchida H. Single- and multiple-dose pharmacokinetics of AM-1155, a new 6-fluoro-8-methoxy quinolone, in humans. Antimicrob Agents Chemother. 1995;39(12):2635–40.
40. Grasela DM. Clinical pharmacology of gatifloxacin, a new fluoroquinolone. Clin Infect Dis. 2000;31(Suppl 2):S51-58.
41. Goa KL, Noble S. Panipenem/betamipron. Drugs. 2003;63(9):913–925; discussion 926.
42. Huth F, Domange N, Poller B, Vapurcuyan A, Durrwell A, Hanna ID, Faller B. Predicting oral absorption for compounds outside the rule of five property space. J Pharm Sci. 2021;110(6):2562–9.
43. Di L, Keefer C, Scott DO, Strelevitz TJ, Chang G, Bi YA, Lai Y, Duckworth J, Fenner K, Troutman MD, Obach RS. Mechanistic insights from comparing intrinsic clearance values between human liver microsomes and hepatocytes to guide drug design. Eur J Med Chem. 2012;57:441–8.
44. Pang KS, Han YR, Noh K, Lee PI, Rowland M. Hepatic clearance concepts and misconceptions: Why the well-stirred model is still used even though it is not physiologic reality? Biochem Pharmacol. 2019;169: 113596.
45. Benet LZ, Sodhi JK. Can in vitro-in vivo extrapolation be successful? recognizing the incorrect clearance assumptions. Clin Pharmacol Ther. 2022;111(5):1022–35.

46. Taniguchi-Takizawa T, Shimizu M, Kume T, Yamazaki H. Benzydamine N-oxygenation as an index for flavin-containing monooxygenase activity and benzydamine N-demethylation by cytochrome P450 enzymes in liver microsomes from rats, dogs, monkeys, and humans. Drug Metab Pharmacokinet. 2015;30(1):64–9.
47. Gantenbein M, Attolini L, Bruguerolle B, Villard PH, Puyoou F, Durand A, Lacarelle B, Hardwigsen J, Le-Treut YP. Oxidative metabolism of bupivacaine into pipecolylxylidine in humans is mainly catalyzed by CYP3A. Drug Metab Dispos. 2000;28(4):383–5.
48. Bertz RJ, Granneman GR. Use of in vitro and in vivo data to estimate the likelihood of metabolic pharmacokinetic interactions. Clin Pharmacokinet. 1997;32(3):210–58.
49. Mangold JB, Gu H, Rodriguez LC, Bonner J, Dickson J, Rordorf C. Pharmacokinetics and metabolism of lumiracoxib in healthy male subjects. Drug Metab Dispos. 2004;32(5):566–71.
50. Zientek M, Jiang Y, Youdim K, Obach RS. In vitro-in vivo correlation for intrinsic clearance for drugs metabolized by human aldehyde oxidase. Drug Metab Dispos. 2010;38(8):1322–7.
51. Bystricky B, Chau I. Patupilone in cancer treatment. Expert Opin Investig Drugs. 2011;20(1):107–17.
52. Weidekamm E, Portmann R, Suter K, Partos C, Dell D, Lucker PW. Single- and multiple-dose pharmacokinetics of fleroxacin, a trifluorinated quinolone, in humans. Antimicrob Agents Chemother. 1987;31(12):1909–14.
53. Stass H, Kubitza D, Halabi A, Delesen H. Pharmacokinetics of moxifloxacin, a novel 8-methoxy-quinolone, in patients with renal dysfunction. Br J Clin Pharmacol. 2002;53(3):232–7.
54. McKeage MJ, Fong PC, Hong X, Flarakos J, Mangold J, Du Y, Tanaka C, Schran H. Mass balance, excretion and metabolism of [(1)(4)C] ASA404 in cancer patients in a phase I trial. Cancer Chemother Pharmacol. 2012;69(5):1145–54.
55. Bergan T. Comparative pharmacokinetics of cefazolin, cephalothin, cephacetril, and cephapirine after intravenous administration. Chemotherapy. 1977;23(6):389–404.
56. Borin MT, Peters GR, Smith TC. Pharmacokinetics and dose proportionality of cefmetazole in healthy young and elderly volunteers. Antimicrob Agents Chemother. 1990;34(10):1944–8.
57. Lenfant B, Namour F, Logeais C, Coussediere D, Rivault O, Bryskier A, Surjus A. Pharmacokinetics of cefodizime following single doses of 0.5, 1.0, 2.0, and 3.0 grams administered intravenously to healthy volunteers. Antimicrob Agents Chemother. 1995;39(9):2037–2041.
58. Shimizu K. Cefoperazone: absorption, excretion, distribution, and metabolism. Clin Ther. 1980;3(Spec Issue):60–79.
59. Brogard JM, Jehl F, Adloff M, Blickle JF, Monteil H. High hepatic excretion in humans of cefpiramide, a new cephalosporin. Antimicrob Agents Chemother. 1988;32(9):1360–4.
60. Peterson LR, Gerding DN, Van Etta LL, Eckfeldt JH, Larson TA. Pharmacokinetics, protein binding, and extravascular distribution of ceftizoxime in normal subjects. Antimicrob Agents Chemother. 1982;22(5):878–81.
61. Gilissen RA, Ferrari L, Barnaby RJ, Kajbaf M. Human hepatic metabolism of a novel 2-carboxyindole glycine antagonist for stroke: in vitro-in vivo correlations. Xenobiotica. 2000;30(9):843–56.
62. Grime K, Paine SW. Species differences in biliary clearance and possible relevance of hepatic uptake and efflux transporters involvement. Drug Metab Dispos. 2013;41(2):372–8.
63. Voigt R, Schroder S, Peiker G. Pharmacokinetic studies of azlocillin and piperacillin during late pregnancy. Chemotherapy. 1985;31(6):417–24.
64. Dieterle W, Faigle JW, Mory H, Richter WJ, Theobald W. Biotransformation and pharmacokinetics of sulfinpyrazone (Anturan) in man. Eur J Clin Pharmacol. 1975;9(2–3):135–45.
65. Pahlman I, Edholm M, Kankaanranta S, Odell M. Pharmacokinetics of Susalimod, a Highly Biliary-excreted Sulphasalazine Analogue, in Various Species. Nonpredictable Human Clearance by Allometric Scaling. Journal of Pharmacy and Pharmacology. 1998;4(10):493–498.
66. He H, Tran P, Yin H, Smith H, Batard Y, Wang L, Einolf H, Gu H, Mangold JB, Fischer V, Howard D. Absorption, metabolism, and excretion of [14C]vildagliptin, a novel dipeptidyl peptidase 4 inhibitor, in humans. Drug Metab Dispos. 2009;37(3):536–44.
67. Dalvie D, Zhang C, Chen W, Smolarek T, Obach RS, Loi CM. Cross-species comparison of the metabolism and excretion of zoniporide: contribution of aldehyde oxidase to interspecies differences. Drug Metab Dispos. 2010;38(4):641–54.